Solid State Ionics 62 (1993) 297–307
North-Holland

SOLID STATE IONICS

Structural characterization of $Li_{1+x}V_3O_8$ insertion electrodes by single-crystal X-ray diffraction

L.A. de Picciotto [1], K.T. Adendorff, D.C. Liles and M.M. Thackeray [2]
Divison of Materials Science and Technology, CSIR, P.O. Box 395, Pretoria 0001, South Africa

Received 2 April 1993; accepted for publication 12 May 1993

The crystal structures of $Li_{1.2}V_3O_8$ and a lithiated product $Li_{4.0}V_3O_8$ have been determined by single-crystal X-ray diffraction methods. The structure refinement of $Li_{1.2}V_3O_8$ confirms that of $Li_{1+x}V_3O_8$ ($x \approx 0$) reported by Wadsley thirty-six years ago. However, unlike Wadsley's data, the refinement of $Li_{1.2}V_3O_8$ demonstrates that the lithium ions are distributed over two independent crystallographic sites. One lithium ion, Li(1), is octahedrally coordinated; the other, Li(2), has tetrahedral coordination. Lithiation of $Li_{1.2}V_3O_8$ with *n*-butyllithium at room temperature displaces Li(1) through an octahedral face into a neighbouring octahedral site, whereas Li(2) shifts its position very slightly to adopt octahedral coordination. During lithiation, the packing of the oxygen-ion array is adjusted slightly to adopt an arrangement that approaches cubic-close-packing. The lithiated product $Li_4V_3O_8$ has a defect rock salt structure. The structural data provide a greater insight into the discharge mechanism that occurs in $Li/Li_{1+x}V_3O_8$ electrochemical cells.

1. Introduction

LiV_3O_8 is one of several vanadium oxides that has received considerable attention as an insertion electrode for rechargeable lithium batteries [1–8]; it can accommodate at least three additional Li^+ ions per formula unit. Pistoia [5] has reported that for a cathode with an initial composition $Li_{1.2}V_3O_8$, lithium is inserted in a single-phase reaction for the range $0 \leq x \leq 1.7$ in $Li_{1.2+x}V_3O_8$, whereas for $1.7 \leq x \leq 3.1$ the reaction is two-phase. Hammou [2] and Raistrick [8] have reported that the single-phase region ends a bit earlier at a composition $Li_{2.5}V_3O_8$.

The structure of $Li_{1+x}V_3O_8$ ($x \approx 0$) has been characterized in detail by Wadsley [9], but little is known about the structures of partially or extensively lithiated products. The difficulty in obtaining structural information about lithiated crystals by profile refinement of powder X-ray or neutron-diffraction patterns can be largely attributed to their complex patterns. These patterns are characterized by peak-overlap because the crystals have low symmetry ($P2_1/m$), and by severe peak-broadening that results from the strain in the lithiated crystals. However, because single crystals of LiV_3O_8 can be synthesised fairly easily, we investigated the possibility of undertaking single-crystal structure analyses of lithiated $Li_{1+x}V_3O_8$ samples. In this paper we report on the synthesis and structural characterization of a $Li_{1.2}V_3O_8$ parent crystal and a lithiated product, $Li_{4.0}V_3O_8$, by single-crystal X-ray diffraction techniques. The data provide information about the phase transitions that occur in $Li_{1.2+x}V_3O_8$ electrodes during discharge of $Li/Li_{1.2+x}V_3O_8$ cells.

2. Experimental

Single crystals of $Li_{1.2}V_3O_8$ were prepared by Wadsley's method by reacting Li_2CO_3 with V_2O_5 in a 1:2 molar ratio in a sealed-quartz ampoule at 680°C for 24 h and allowing the ampoule to cool slowly, undisturbed, in the furnace [9]. Although many of the crystals were badly twinned, a single crystal of dimensions $0.26 \times 0.10 \times 0.07$ mm that was suitable for data collection was isolated from the matrix. Crys-

[1] Present address: Dirart S.A., Via Campo Marzio 11, 6900 Lugano, Switzerland.
[2] Author to whom correspondence should be addressed.

tals of $Li_{1.2}V_3O_8$ were lithiated by reaction with a 0.46 M solution of *n*-butyllithium in hexane at 20°C for seven days. The lithium content in the parent compound and in the lithiated product was determined by atomic absorption spectroscopy. The compositions of the parent compound, $Li_{1.2}V_3O_8$, and the lithiated product, $Li_{4.0}V_3O_8$, are consistent with samples prepared elsewhere [5,10]. Although many of the crystals had fractured during the lithiation reaction, it was possible to extract a single crystal of $Li_{4.0}V_3O_8$ with dimensions $0.15\times0.09\times0.06$ mm for data collection.

To check the reversibility of the lithiation reaction, lithium was extracted from $Li_{4.0}V_3O_8$ at 20°C by using a slight excess of Br_2 (0.125 M solution of Br_2 in $CHCl_3$) according to the reaction:

$$Li_4V_3O_8 + y/2Br_2 \rightarrow Li_{4-y}V_3O_8 + yLiBr\,.$$

The sample was reacted for five days and thereafter washed in $CHCl_3$ and EtOH.

Powder X-ray diffraction patterns were recorded on an automated Rigaku diffractometer with Cu Kα radiation ($\lambda = 1.54178$ Å) monochromated by a graphite single crystal. Calculated X-ray powder patterns were generated with the program LAZY PULVERIX [11]. Single-crystal X-ray diffraction data were collected on a Philips PW1100 diffractometer with graphite-crystal-monochromated Mo Kα radiation ($\lambda = 0.7107$ Å). Unit cell dimensions of $Li_{1.2}V_3O_8$ and $Li_{4.0}V_3O_8$ were determined from least-squares refinements of the angular settings of 25 and 20 high-order reflections, respectively. The diffractometer settings for the two data collections, the crystal data and refinement parameters of $Li_{1.2}V_3O_8$ and $Li_{4.0}V_3O_8$ are given in table 1. Note that there are alternative settings for the monoclinic unit cells of $Li_{1.2}V_3O_8$ and $Li_{4.0}V_3O_8$; the alternative unit cells

Table 1
Diffractometer settings, crystal data and refinement parameters for $Li_{1.2}V_3O_8$ and $Li_{4.0}V_3O_8$.

Diffractometer settings	$Li_{1.2}V_3O_8$	$Li_{4.0}V_3O_8$
θ-range (°)	3–25	3–23
Scan mode	ω–2θ	ω–2θ
Scan speed (°/s)	0.040	0.033
Scan width (°)	1.8	1.5
Detector aperture:		
horizontal (°)	2	2
vertical (°)	1	1
Total number of reflections	569	444

Crystal data	(i)	(ii) (alternative setting)	(i)	(ii) (alternative setting)
Space group symmetry	$P2_1/m$	$P2_1/m$	$P2_1/m$	$P2_1/m$
a (Å)	6.596	6.596	5.955	5.955
b (Å)	3.559	3.559	3.911	3.911
c (Å)	11.862	11.695	11.915	11.656
β (°)	107.66	104.85	107.03	102.20
Volume (Å^3)	265.36	265.36	265.33	265.33
Z	2	2	2	2
ϱ (calc) (g/cm^3)	3.62	3.62	3.86	3.86

Refinement parameters		
$R[=\Sigma\|\Delta F\|/\Sigma F_{obs}]$	0.0353	0.1438
$R_G[=(\Sigma\|\Delta F\|^2/\Sigma F^2_{obs})^{1/2}]$	0.0470	0.1240
Number of variables	73	76
Number of reflections used	560	444

have slightly smaller c and β values. Background radiation was counted for half the scan time on each side of a reflection. Reflections were considered to be absent if $I_{rel} < 1.65\sigma(I_{rel})$, where $\sigma(I_{rel}) = [(0.02S)^2 + S + B]^{1/2}$, S=scan count and B=background count. Three reflections were measured every 30 min to monitor the stability of the crystals during the data collection. $Li_{1.2}V_3O_8$ crystals showed no signs of any significant decomposition whereas the intensities of the three reference reflections of $Li_{4.0}V_3O_8$ were on average 7% less at the end of the data collection. Intensities were corrected for Lorentz and polarization effects but not for absorption. Structures were refined with the computer program SHELX-76 [12]. Scattering factor amplitudes for the atoms were those of Cromer and Waber [13].

3. Structure refinements

3.1. $Li_{1.2}V_3O_8$

The structure of $Li_{1.2}V_3O_8$ was initially refined with the atomic coordinates of LiV_3O_8 reported by Wadsley [9]. The refined coordinates were in excellent agreement with Wadsley's data which reflects the accuracy of the structure determination that was achieved with intensity data from multiple-film Weissenberg photographs thirty six years ago. A difference Fourier map calculated at the end of the refinement indicated that the lithium ions were distributed over two crystallographically-independent sites in the structure. The thermal parameters of the three vanadium and eight oxygen ions were refined anisotropically. Li(1) was refined isotropically; Li(2) was assigned the same thermal parameter as Li(1). The good fit between observed and calculated data was reflected by a final R factor of 3.5%. Unit weights ware assigned to all the reflections. The atomic coordinates and thermal parameters of $Li_{1.2}V_3O_8$ are given in table 2.

3.2. $Li_{4.0}V_3O_8$

Because the unit cell parameters of $Li_{1.2}V_3O_8$ and $Li_{4.0}V_3O_8$ were similar and the unit cell volumes almost identical (table 1), the possibility existed that only minor structural modifications occurred to the V_3O_8 framework of the structure during lithiation – a hypothesis that proved to be correct in the structure determination of $Li_{4.0}V_3O_8$. The atomic coordinates of the three "heavy" vanadium ions in $Li_{1.2}V_3O_8$ were used in the initial least-squares refinement to calculate a set of phases of the diffracted X-rays from which the remainder of the structure of $Li_{4.0}V_3O_8$ was solved. Successive difference Fourier maps revealed the positions of the oxygen ions and three of the four Li^+ ions in the structure. The remaining Li^+ ion was assumed to be distributed over two interstitial octahedral sites located at approxi-

Table 2
Fractional atomic coordinates of $Li_{1.2}V_3O_8$.

Atoms	x/a	y/b	z/c	U_{11}	U_{22}	U_{33}	U_{13} [a]
V(1)	0.8426(2)	0.25	0.5365(1)	0.0078(7)	0.0049(7)	0.0050(7)	0.0029(5)
V(2)	0.2038(2)	0.25	0.0778(1)	0.0086(7)	0.0041(7)	0.0054(7)	0.0016(5)
V(3)	0.0688(2)	0.25	0.8034(1)	0.0102(7)	0.0060(7)	0.0058(7)	0.0040(5)
Li(1)	0.501(3)	0.25	0.683(2)	0.028(4)	–	–	–
Li(2) [b]	0.570(30)	0.25	0.050(17)	0.028	–	–	–
O(1)	0.0687(9)	0.25	0.4600(5)	0.012(3)	0.010(3)	0.011(3)	0.008(2)
O(2)	0.8829(9)	0.25	0.9293(5)	0.012(3)	0.011(3)	0.008(3)	0.005(2)
O(3)	0.7986(9)	0.25	0.6710(5)	0.012(3)	0.013(3)	0.007(3)	0.005(2)
O(4)	0.4161(10)	0.25	0.1856(5)	0.012(3)	0.026(4)	0.011(3)	0.000(2)
O(5)	0.6161(10)	0.25	0.4394(5)	0.012(3)	0.024(4)	0.008(3)	0.002(2)
O(6)	0.2885(9)	0.25	0.9553(5)	0.010(3)	0.019(3)	0.007(3)	0.003(2)
O(7)	0.2227(9)	0.25	0.7237(5)	0.010(3)	0.018(3)	0.012(3)	0.004(2)
O(8)	0.9861(9)	0.25	0.1752(5)	0.011(3)	0.014(3)	0.006(3)	0.003(2)

[a] $U_{12} = U_{23} = 0.0$.
[b] Site occupancy of Li(2) = 0.10(5).

Table 3
Fractional atomic coordinates of $Li_{4.0}V_3O_8$.

Atoms	x/a	y/b	z/c	U_{11}	U_{22}	U_{33}	U_{13} [a]
V(1)	0.8680(11)	0.25	0.5446(4)	0.0681(41)	0.031(3)	0.014(3)	0.043(3)
V(2)	0.1888(10)	0.25	0.0774(4)	0.053(4)	0.021(3)	0.014(3)	0.012(3)
V(3)	0.0492(10)	0.25	0.8059(4)	0.042(3)	0.033(3)	0.014(3)	0.007(2)
Li(1)	0.289(12)	0.25	0.333(6)	0.055(17)	-	-	-
Li(2)	0.648(8)	0.25	0.061(4)	0.020(10)	-	-	-
Li(3)	0.775(13)	0.25	0.310(7)	0.062(19)	-	-	-
Li(4)	Atom not located in a difference Fourier map [b]						
O(1)	0.074(4)	0.25	0.451(2)	0.046(13)	0.057(16)	0.019(11)	0.002(9)
O(2)	0.876(4)	0.25	0.933(1)	0.049(13)	0.030(12)	0.000(9)	0.008(8)
O(3)	0.766(5)	0.25	0.685(2)	0.093(19)	0.037(13)	0.003(9)	0.008(10)
O(4)	0.452(5)	0.25	0.179(2)	0.122(23)	0.041(14)	0.018(11)	0.039(13)
O(5)	0.617(3)	0.25	0.443(1)	0.023(10)	0.034(12)	0.013(9)	0.003(7)
O(6)	0.305(3)	0.25	0.946(2)	0.036(11)	0.043(13)	0.017(10)	0.011(9)
O(7)	0.213(4)	0.25	0.701(2)	0.053(13)	0.031(12)	0.021(10)	0.027(9)
O(8)	0.972(4)	0.25	0.177(2)	0.059(15)	0.045(14)	0.003(9)	0.014(9)

[a] $U_{12}=U_{23}=0.0$.
[b] Assumed to be distributed over two interstitial octahedral sites: $S_o(1)$ at 0.406, 0.25, 0.566 and $S_o(2)$ at 0.543, 0.25, 0.818.

mately (0.406 0.25 0.566) and (0.543 0.25 0.818). Vanadium and oxygen ions were refined with anisotropic thermal parameters. Isotropic temperature factors were assigned to the lithium ions. The final R factor was 14.4%. Unit weights were assigned to all reflections. The relatively high value of R can be attributed to the lower quality X-ray data of $Li_{4.0}V_3O_8$ compared to the data of the parent $Li_{1.2}V_3O_8$. The intensity data was characterized, in particular, by severe broadening of the individual diffraction peaks as a result of strain that had been induced into the crystal by the lithium insertion reaction. Nevertheless, the data was of sufficient high quality to provide an accurate description of the $Li_{4.0}V_3O_8$ structure.

4. Results and discussion

4.1. The structures of $Li_{1.2}V_3O_8$ and $Li_{4.0}V_3O_8$

4.1.1. $Li_{1.2}V_3O_8$

A [010] projection of the $Li_{1.2}V_3O_8$ structure as determined from diffractometer data is shown in fig. 1a. The atomic labelling, which is the same as that used by Wadsley [9] is given in fig. 2a. A stereoscopic illustration of the structure is provided in fig. 3a. The structure refinement of $Li_{1.2}V_3O_8$ showed that

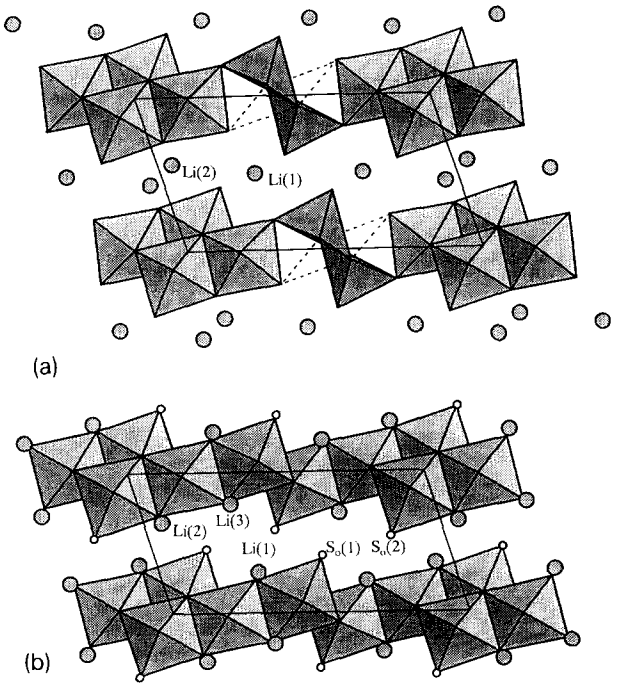

Fig. 1. (a) $Li_{1.2}V_3O_8$ ([100] projection). VO_5 and VO_6 coordination polyhedra are shown. Shaded circles indicate the lithium positions. Broken lines complete the coordination octahedra for V(1); (b) $Li_{4.0}V_3O_8$ ([100] projection). VO_6 coordination octahedra are shown. Shaded circles indicate the lithium positions. Small open circles indicate probable octahedral sites for the 4th (undetected) lithium ion.

the Li^+ ions reside predominantly in an octahedral site, labelled Li(1) (site occupancy = 1.0), and that the excess lithium occupies one crystallographically-independent tetrahedral site, labelled Li(2) (site occupancy = 0.10(5)). The refined composition, $Li_{1.1}V_3O_8$, was therefore in good agreement with the chemically-determined composition. The final difference Fourier map showed that the interstitial tetrahedral sites $S_t(1)$, $S_t(2)$ and $S_t(3)$ in fig. 2a did not contain any detectable lithium. Wadsley could only detect lithium in the octahedral site; he selected three of the crystallographically-independent tetrahedral sites Li(2), $S_t(1)$ and $S_t(2)$ as possible alternative sites for additional lithium ions in $Li_{1+x}V_3O_8$ structures.

The remainder of the structure confirms the description that has been given previously [9]. It is worthwhile to repeat the description in this paper because of its relation to the lithiated phase, $Li_{4.0}V_3O_8$. Two of the vanadium ions, V(2) and V(3), are octahedrally coordinated; the third crystallographically-independent vanadium ion, V(1), has trigonal bi-pyramidal coordination. The V_3O_8 framework is comprised of two structural units, firstly, double chains of edge-shared VO_6 octahedra and, secondly, double chains of edge-shared trigonal bi-pyramids

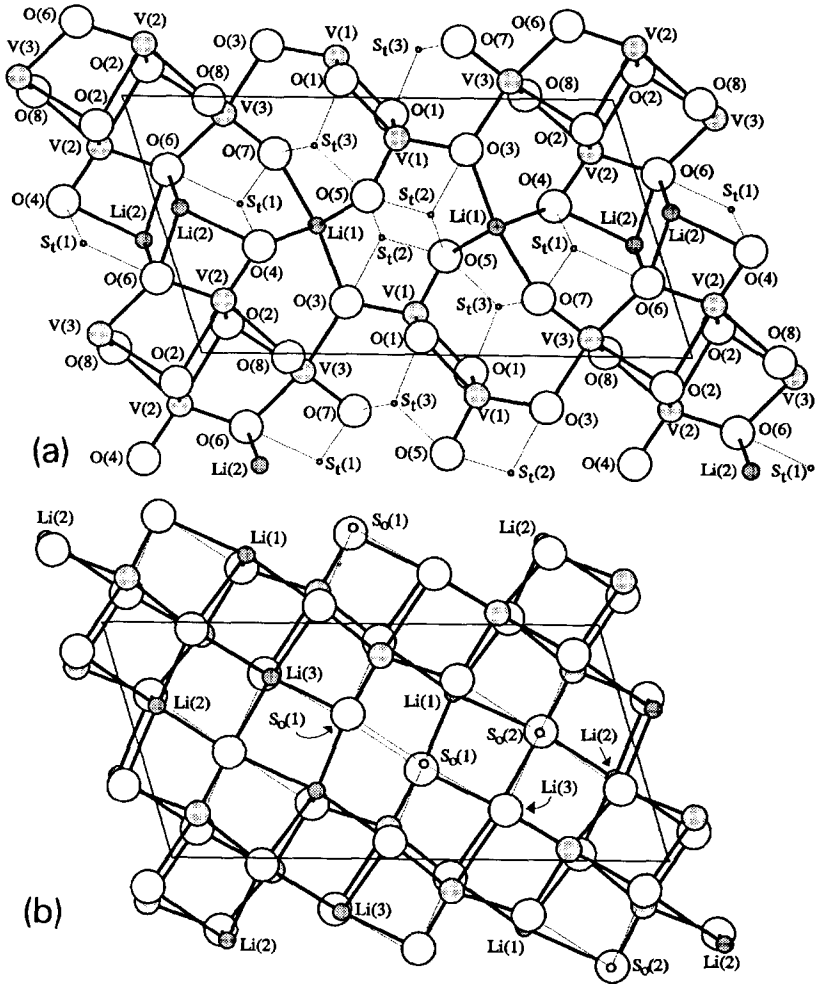

Fig. 2. (a) $Li_{1.2}V_3O_8$ ([100] projection) showing the atom labelling; (b) $Li_{4.0}V_3O_8$ ([100] projection). V and O atoms are labelled as in (a). The arrows indicate atoms (or sites) hidden by O atoms.

(fig. 1a). The chains of octahedra and trigonal bipyramids are linked by corner-shared oxygens, O(3), to provide continuous puckered sheets of VO_n ($n=5$, 6) polyhedra. (If a sixth, long V(1)–O(7) bond of 2.800(6) Å is considered as part of the coordination sphere, shown by the dotted line in fig. 1a, then V(1) may be regarded as having octahedral coordination.) In addition to the tetrahedral sites shown in fig. 2a, the interstitial space of the V_3O_8 framework contains several distorted octahedra that share faces with the tetrahedra. A two-dimensional network of interlinked tetrahedra and octahedra therefore exists for Li^+-ion transport between the sheets of VO_n polyhedra. It should be noted, however, that although the oxygen ions in $Li_{1.2}V_3O_8$ may be regarded as forming a distorted close-packed array, the layers for Li^+-ion transport are not parallel to the close-packed oxygen planes as they are in other well-known layered compounds such as $LiVO_2$ [14], $LiNiO_2$ [15] and $LiCoO_2$ [16].

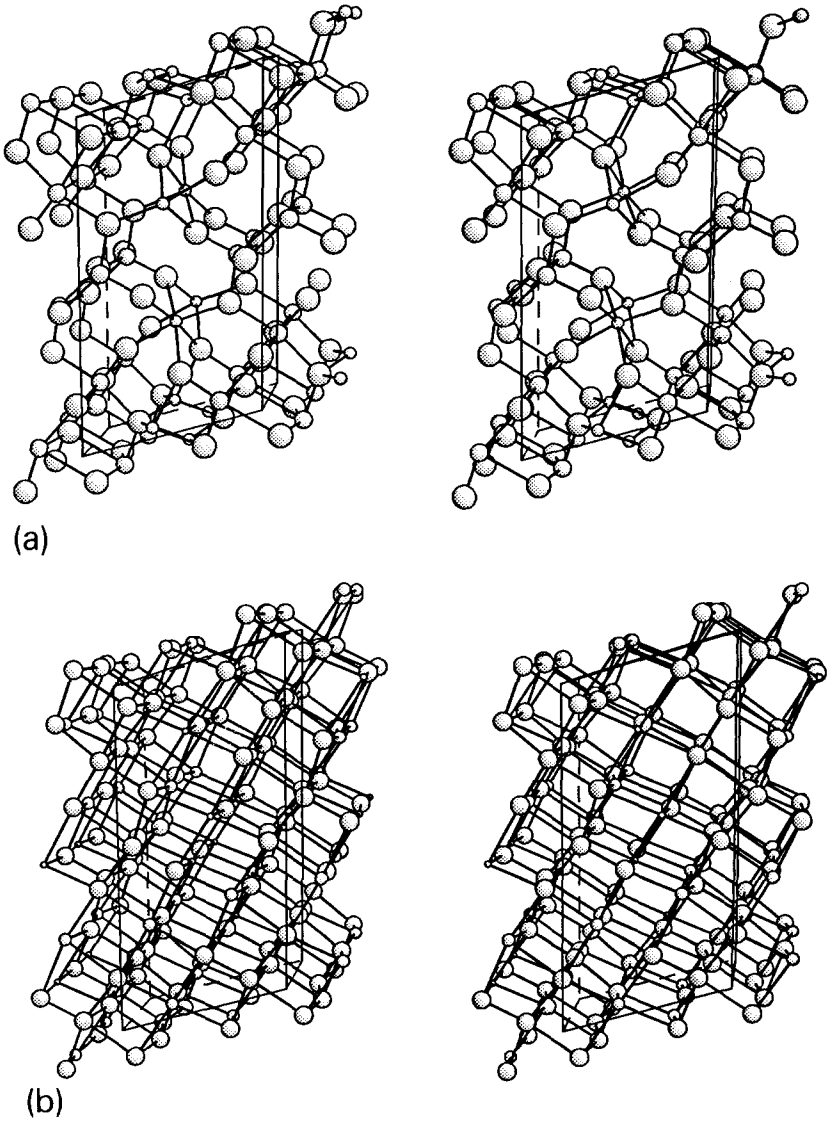

Fig. 3. (a) Stereoscopic projection ([010]) of $Li_{1.2}V_3O_8$; (b) Stereoscopic projection [(010)] of $Li_{4.0}V_3O_8$.

Interatomic V–O and Li–O distances in $Li_{1.2}V_3O_8$ are listed in table 4. The VO_5 trigonal bi-pyramid and each of the two VO_6 octahedra have one significantly short V–O bond, namely, V(1)–O(5) = 1.586(6) Å, V(2)–O(4) = 1.584(6) Å and V(3)–O(7) = 1.583(6) Å. This phenomenon is well-known in other vanadium oxides, particularly those with compositions between VO_2 and V_2O_5 [17]. The V–O distance opposite the short bond is long; in the two octahedra these bonds are V(2)–O(2) = 2.307(6) Å and V(3)–O(2) = 2.201(6) Å. The V(1)–O(7) distance of 2.800(6) Å puts O(7) outside the coordination sphere of the trigonal bi-pyramid; if included, V(1) adopts octahedral coordination, as previously stated.

The six Li(1)–O octahedral distances vary between 2.01(2) Å and 2.32(2) Å, whereas the four Li(2)–O tetrahedral distances vary between 1.85(19) Å and 2.15(19) Å. It is significant to note that if the two next-nearest oxygen neighbours of Li(2) are brought into the coordination sphere (Li(2)–O(2) = 2.86(20) Å and Li(2)–O(8) = 2.74(18) Å), then Li(2) adopts octahedral coordination. In fact, only a very small displacement is required to move Li(2) from the tetrahedral site to the centre of the octahedron as illustrated in fig. 4a.

A [100] projection of the $Li_{1.2}V_3O_8$ structure is given in fig. 5a. The double chains of edge-shared VO_5 trigonal bi-pyramids that link the VO_6 octahedra by corner-shared oxygens are clearly visible. This projection also demonstrates that the layers of oxygen ions defined by the {104} crystallographic planes, deviate slightly from cubic-close-packing. If O(7) is considered to be bonded to V(1) to give V(1) octahedral coordination, then the V_3O_8 framework of $Li_{1.2}V_3O_8$ may be regarded as having a defect rock salt structure. It is important to note that the Li(1) ions are located in octahedral sites not normally associated with the interstitial octahedral sites of a defect rock salt structure; however, both Li(1) and Li(2) can move into the octahedral sites of a rock salt structure by small displacements as shown in figs. 4a and 5a.

Table 4
V–O and Li–O distances (Å) in $Li_{1.2}V_3O_8$.

V–O distances					
Trigonal Bi-pyramidal		Octahedral			
		(i)		(ii)	
V(1)–O(1)	1.870(2)	V(2)–O(2)	1.863(2)	V(3)–O(2)	2.201(6)
V(1)–O(1)	1.870(2)	V(2)–O(2)	1.863(2)	V(3)–O(3)	1.986(6)
V(1)–O(1)	1.967(6)	V(2)–O(2)	2.307(6)	V(3)–O(6)	1.940(6)
V(1)–O(3)	1.706(6)	V(2)–O(4)	1.584(6)	V(3)–O(7)	1.583(6)
V(1)–O(5)	1.586(6)	V(2)–O(6)	1.708(6)	V(3)–O(8)	1.849(2)
		V(2)–O(8)	2.099(6)	V(3)–O(8)	1.849(2)
[V(1)–O(7)	2.800(6)] [a]				

Li–O distances			
Octahedral		Tetrahedral	
Li(1)–O(3)	2.01(2)	Li(2)–O(4)	2.15(19)
Li(1)–O(4)	2.32(1)	Li(2)–O(6)	1.85(19)
Li(1)–O(4)	2.32(1)	Li(2)–O(6)	2.03(10)
Li(1)–O(5)	2.28(1)	Li(2)–O(6)	2.03(10)
Li(1)–O(5)	2.28(1)		
Li(1)–O(7)	2.03(2)	[Li(2)–O(2)	2.86(20)] [b]
		[Li(2)–O(8)	2.74(18)] [b]

[a] If included in the coordination sphere V(1) would have octahedral coordination.
[b] If included in the coordination sphere Li(2) would have octahedral coordination.

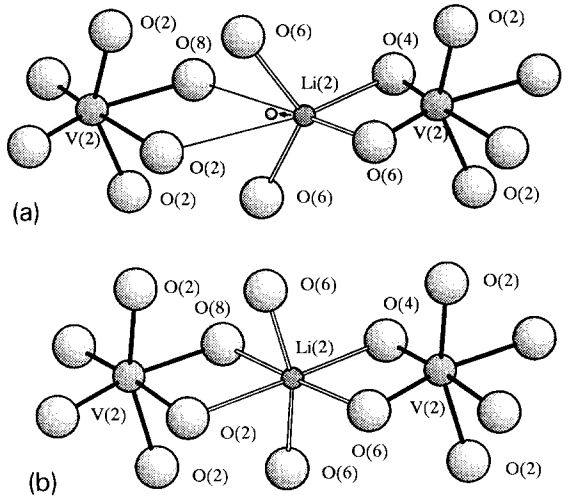

Fig. 4. (a) The environment around Li(2) in $Li_{1.2}V_3O_8$. The arrow indicates the displacement necessary for Li(2) to move to the mean position for octahedral coordination; (b) The environment around Li(2) in $Li_{4.0}V_3O_8$.

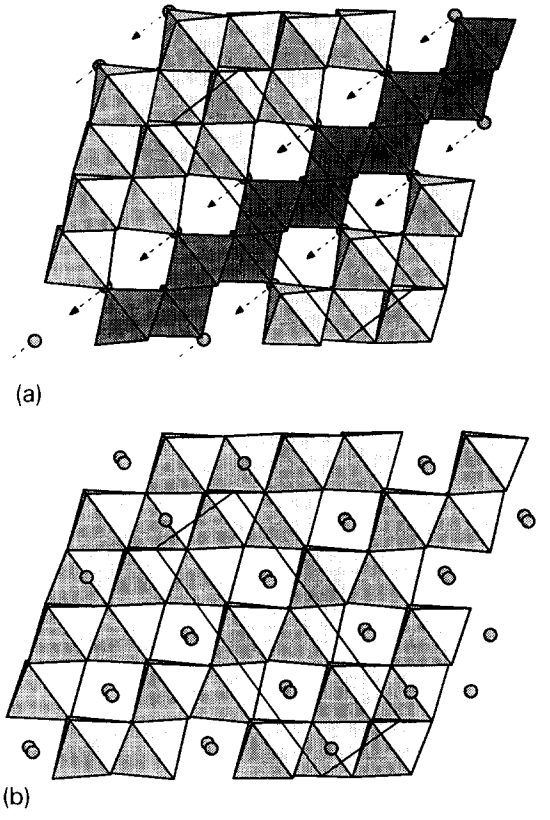

Fig. 5. $Li_{1.2}V_3O_8$ ([100] projection). The {014} planes, representing planes of approximately close packed oxygen ions, are horizontal. The darker shaded polyhedra are the VO_5 trigonal bipyramids. The arrows show the movement of Li(1) to the interstitial octahedral sites of a defect rock salt structure; (b) $Li_{4.0}V_3O_8$ ([100] projection). The oxygen ion array approaches ideal cubic-close-packing.

4.1.2. $Li_4V_3O_8$

The structure of $Li_{4.0}V_3O_8$ is closely related to $Li_{1.2}V_3O_8$. Illustrations of the structure of $Li_{4.0}V_3O_8$ that correspond to those of $Li_{1.2}V_3O_8$ in figs. (1–5)a are shown in figs. (1–5)b. The defect rock salt character of $Li_{4.0}V_3O_8$ is clearly evident in these illustrations. The transformation from the parent $Li_{1.2}V_3O_8$ structure to the defect rock salt phase includes the following structural modifications:

(1) The oxygen ions undergo minor displacements to adopt an arrangement which is significantly closer to ideal cubic-close-packing than it is in the parent compound;

(2) the vanadium ions are not displaced by the incoming lithium ions. Of particular significance, however, is the shortening of the V(1)–O(7) distance of 2.800(6) Å in $Li_{1.2}V_3O_8$ to 2.337(18) Å in $Li_{4.0}V_3O_8$ which changes the coordination of V(1) from trigonal bi-pyramidal to octahedral coordination (table 5). The interatomic distances in tables 4 and 5 show that the VO_6 octahedra in $Li_{4.0}V_3O_8$ are not as distorted as they are in $Li_{1.2}V_3O_8$;

(3) the octahedrally coordinated Li(1) ions in $Li_{1.2}V_3O_8$ are displaced during lithiation via an octahedral face into neighbouring octahedra (figs. 5a,b). Li(1) ions in $Li_{1.2}V_3O_8$ (fig. 2a) can take up either the positions Li(1) or Li(3) in $Li_{4.0}V_3O_8$ (fig. 2b);

(4) the tetrahedrally coordinated Li(2) ions undergo a small displacement to move to octahedral coordination (see figs. 4a,b). Fig. 4b shows that the LiO_6 octahedra link VO_6 octahedra by sharing common edges, a feature which is characteristic of rock salt-type structures;

(5) lithiation of $Li_{1.2}V_3O_8$ is accompanied by a significant contraction of a from 6.596 Å to 5.955 Å which is a manifestation of the increase in binding energy provided by the inserted lithium ions; the sheets of VO_6 octahedra are therefore closer to one another in $Li_4V_3O_8$ than in $Li_{1.2}V_3O_8$ as shown in fig. 1a and b which have been drawn on the same scale. The contraction of a is offset by the lengthening of

Table 5
V–O and Li–O distances (Å) in $Li_{4.0}V_3O_8$.

V–O octahedral distances					
V(1)-O(1)	1.984(4)	V(2)-O(2)	1.990(4)	V(3)-O(2)	2.067(22)
V(1)-O(1)	1.984(4)	V(2)-O(2)	1.990(4)	V(3)-O(3)	1.870(21)
V(1)-O(1)	1.889(26)	V(2)-O(2)	2.137(17)	V(3)-O(6)	1.901(17)
V(1)-O(3)	1.935(24)	V(2)-O(4)	1.674(25)	V(3)-O(7)	1.794(24)
V(1)-O(5)	1.625(16)	V(2)-O(6)	1.893(23)	V(3)-O(8)	1.974(3)
V(1)-O(7)	2.337(18)	V(2)-O(8)	1.993(25)	V(3)-O(8)	1.974(3)
Li–O octahedral distances [a]					
Li(1)-O(1)	2.16(8)	Li(2)-O(2)	2.31(6)	Li(3)-O(1)	2.06(7)
Li(1)-O(3)	1.98(1)	Li(2)-O(4)	2.08(6)	Li(3)-O(4)	2.09(7)
Li(1)-O(3)	1.98(1)	Li(2)-O(6)	1.98(1)	Li(3)-O(5)	2.06(9)
Li(1)-O(4)	2.31(8)	Li(2)-O(6)	1.98(1)	Li(3)-O(7)	1.96(1)
Li(1)-O(5)	2.01(6)	Li(2)-O(6)	2.10(4)	Li(3)-O(7)	1.96(1)
Li(1)-O(8)	2.22(6)	Li(2)-O(8)	2.02(4)	Li(3)-O(8)	2.23(9)

[a] Li(4) not located in structure.

b and *c* to give $Li_{4.0}V_3O_8$ the same unit cell volume (265 Å^3) as $Li_{1.2}V_3O_8$ (table 1).

4.2. Powder X-ray diffraction patterns

The observed powder X-ray diffraction patterns of $Li_{1.2}V_3O_8$ and $Li_{4.0}V_3O_8$ and calculated patterns derived from the single crystal X-ray data in tables 1, 2 and 3 are shown in fig. 6a–d. The slight mismatch between the observed and calculated patterns of the two samples, in terms of both peak position and intensity, is attributed to a non-uniform composition of the individual crystallites in the powdered samples. The X-ray pattern of a chemically-delithiated product $Li_{4-y}V_3O_8$ ($y \approx 3$) is given in fig. 6e. The extremely strong {100} peak at approximately 14° 2θ in the observed patterns of $Li_{1.2}V_3O_8$ and $Li_{4-y}V_3O_8$ (fig. 6a, e) is attributed to preferred orientation of the crystals in the sample holder. This is not unexpected because the {100} crystallographic planes correspond to the layers of VO_n polyhedra (fig. 1a). The preferred orientation is not as pronounced in the observed pattern of the lithiated phase (fig. 6c). The X-ray patterns of $Li_{1.2}V_3O_8$ (fig. 6a) and $Li_{4.0}V_3O_8$ (fig. 6c) are significantly different, despite the small differences in atomic coordinates and unit cell volumes. The changes in peak positions can be mainly attributed to the changes in the *a* and *b* lattice parameters which contract and expand, respectively, by approximately 10%. $Li_{4.0}V_3O_8$ is less crystalline than $Li_{1.2}V_3O_8$, which can be expected for a product of a lithium-insertion reaction.

The X-ray pattern of the chemically-delithiated product (fig. 6e) is similar to that of $Li_{1.2}V_3O_8$ (fig. 6a) but shows differences in the relative intensities of the peaks; it also shows, somewhat surprisingly, that on delithiation a highly crystalline structure is regenerated. These observations therefore confirm the reversibility of the lithiation reaction, but indicate that the structure of the delithiated product is a slight modification of the parent structure.

4.3. The transition of $Li_{1.2}V_3O_8$ to $Li_{4.0}V_3O_8$

It has been previously reported that the powder X-ray diffraction patterns of $Li_{1.2+x}V_3O_8$ compounds are similar for the range $0 \leq x \leq 1.7$, but that for $x > 1.7$ a significant change in the X-ray pattern is observed [5]. Electrochemical studies of Li/$Li_{1.2+x}V_3O_8$ cells have demonstrated that the open-circuit-voltage drops rapidly from 3.70 V to 2.85 V over the range $0 \leq x \leq 0.8$; the voltage drops more slowly over the range $0.8 \leq x \leq 1.7$, from 2.85 V to 2.70 V. Thereafter, the cells discharge at constant voltage (2.7 V) to $x = 3.1$ [5]. Combining this information with the structural data obtained in this study, the lithium-insertion reaction

$$2.8\mathrm{Li} + \mathrm{Li}_{1.2}\mathrm{V}_3\mathrm{O}_8 \rightarrow \mathrm{Li}_{4.0}\mathrm{V}_3\mathrm{O}_8$$

can be described as follows:
Lithium is inserted into the interstitial space of the $Li_{1.2+x}V_3O_8$ structure in two single-phase reaction processes. For $0 \leq x \leq 0.8$, lithium is inserted into the tetrahedral sites Li(2). These sites are fully occupied when the composition reaches $Li_2V_3O_8$ ($x=0.8$). The limited changes in the X-ray pattern over this compositional range suggest that Li(2) remains tetrahedrally coordinated and is not displaced to adopt octahedral coordination. For $0.8 \leq x \leq 1.7$, lithium is

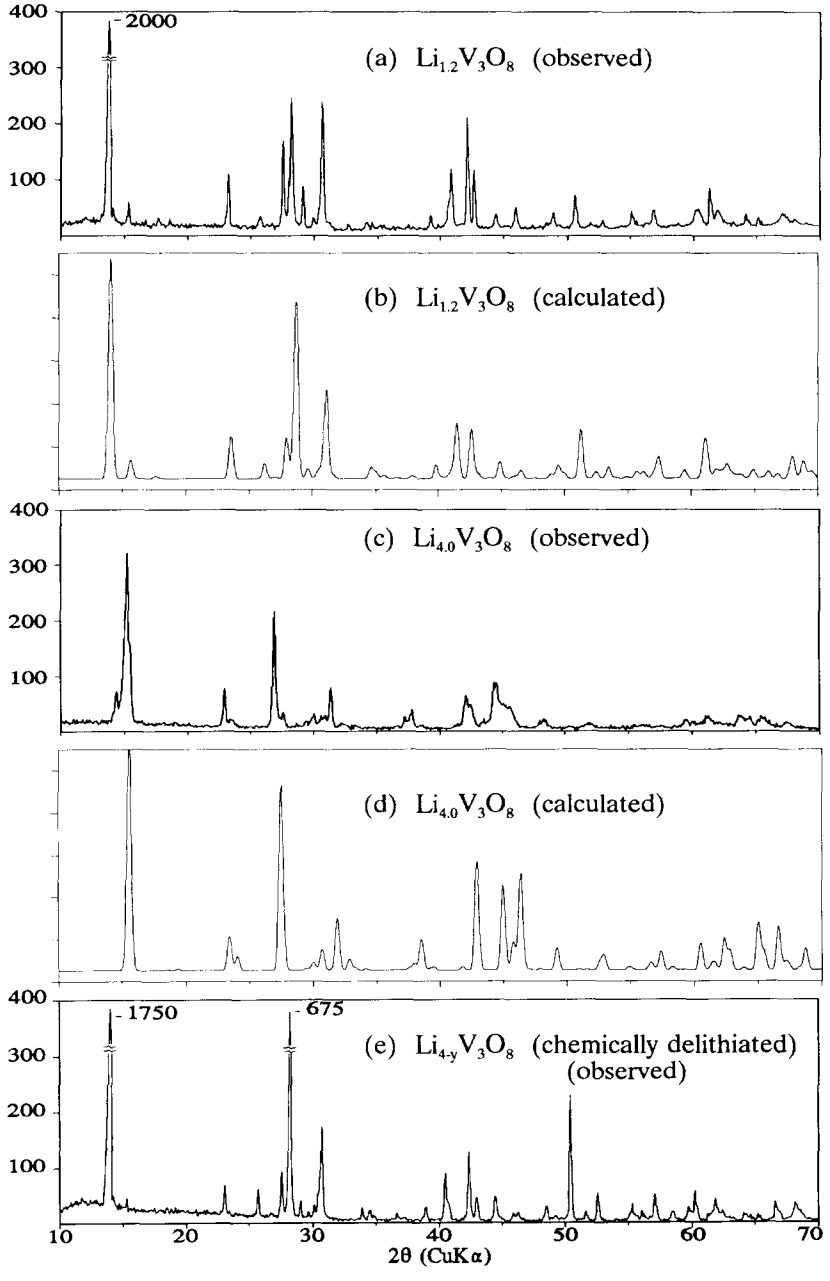

Fig. 6. Observed and calculated powder X-ray diffraction patterns.

inserted into the interstitial space of the $Li_2V_3O_8$ structure. Further crystallographic data is necessary, however, to determine the exact sites in which the additional 0.9 Li^+ ions are located; it is possible that they are distributed over the tetrahedral sites $S_t(1)$ and $S_t(2)$ in fig. 2a, as predicted by Wadsley [9].

At $x \approx 1.7$, the Li(1) ions in the octahedral sites are displaced by the incoming lithium ions into neighbouring octahedral sites (Li(1) and Li(3) in fig. 2b). This displacement which is accompanied by a shortening of the V–O bond distances due to the reduction of the vanadium ions modifies the oxygen-ion array towards cubic-close-packing and that generates the defect rock salt phase. For $1.7 \leq x \leq 2.8$, lithium ions are accommodated in the octahedral sites of the structure and predominantly in sites Li(1), Li(2) and Li(3) (fig. 2b); the fourth lithium ion is distributed between the two remaining octahedral sites, $S_o(1)$ and $S_o(2)$. The reaction observed for $1.7 \leq x \leq 2.8$ in the electrochemical curve is therefore attributed to the coexistence of two phases; one is $Li_{2.9}V_3O_8$ with Li(1) in the octahedral sites of the parent $Li_{1.2}V_3O_8$ compound and the remaining lithium in tetrahedral sites, and the second is a defect rock salt structure with a nominal composition $Li_{4.0}V_3O_8$.

5. Conclusions

The crystal structures of $Li_{1.2}V_3O_8$ and $Li_{4.0}V_3O_8$ have been determined by single-crystal X-ray diffraction. The study has provided greater clarity about the discharge reaction of $Li/Li_{1+x}V_3O_8$ electrochemical cells. The phase transition of $Li_{2.9}V_3O_8$ to the rock salt phase $Li_{4.0}V_3O_8$ that occurs with a concomitant contraction of the a lattice parameter and an expansion of b and c appears to be the reason for the deterioration in the rechargeability of $Li/Li_{1.2+x}V_3O_8$ cells when x exceeds 1.7, despite a negligible change in unit cell volume. Further work is required to establish exactly which interstitial sites in the unit cell are occupied by lithium at intermediate compositions between $Li_{1.2}V_3O_8$ and $Li_{4.0}V_3O_8$. In principle, it should be possible to lithiate $Li_{1+x}V_3O_8$ to the stoichiometric rock salt composition $Li_5V_3O_8$ under carefully-controlled reaction conditions.

Acknowledgement

M. Schatz is thanked for undertaking the atomic absorption analyses.

References

[1] F. Bonino, M. Ottaviani, B. Scrosati and G. Pistoia, J. Electrochem. Soc. 135 (1988) 12.
[2] A. Hammou and A. Hammouche, Electrochim. Acta 33 (1988) 1719.
[3] M. Pasquali, G. Pistoia, V. Manev and R.V. Moshtev, J. Electrochem. Soc. 133 (1986) 2454.
[4] G. Pistoia, M. Pasquali, M. Tocci, V. Manev and R.V. Moshtev, J. Power Sources 15 (1985) 13.
[5] G. Pistoia, M. Pasquali, M. Tocci, R.V. Moshtev and V. Manev, J. Electrochem. Soc. 132 (1985) 281.
[6] G. Pistoia, S. Panero, M. Tocci, R.V. Moshtev and V. Manev, Solid State Ionics 13 (1984) 311.
[7] K. Nassau and D.W. Murphy, J. Non-Cryst. Solids 44 (1981) 297.
[8] I.D. Raistick, Rev. Chim. Miner. 21 (1984) 456.
[9] A.D. Wadsley, Acta Cryst. 10 (1957) 261.
[10] K. West, B. Zachau-Christiansen, M.J.L. Ostergard and T. Jacobsen, J. Power Sources 20 (1987) 165.
[11] K. Yvon, W. Jeitschko and E. Parthe, J. Appl. Cryst. 10 (1977) 73.
[12] G.M. Sheldrick, in: Computing in Crystallography, (Delft University Press, Delft, 1978) p. 34.
[13] D.T. Cromer and J.T. Waber, International Tables for X-ray Crystallography, Vol. IV (Kynoch Press, Birmingham, 1974) p. 71.
[14] L.A. de Picciotto, M.M. Thackeray, W.I.F. David, P.G. Bruce and J.B. Goodenough, Mat. Res. Bull. 19 (1984) 1497.
[15] J.R. Dahn, U. von Sacken and C.A. Michal, Solid State Ionics 44 (1990) 87.
[16] K. Mizushima, P.C. Jones, P.J. Wiseman and J.B. Goodeneough, Mat. Res. Bull. 15 (1980) 783.
[17] A.F. Wells, in: Structural Inorganic Chemistry (Clarendon Press, Oxford, 1975) p. 467.